A CAPACITY-BASED SEISMIC DAMAGE INDEX FOR REINFORCED CONCRETE STRUCTURAL MEMBERS

S. Shiradhonkar[1], R. Sinha[2]

[1] *Former Doctoral student, Department of Civil Engineering, Indian Institute of Technology Bombay, Mumbai-76, saurabh.coep@gmail.com*

[2] *Professor, Department of Civil Engineering, Indian Institute of Technology Bombay, Mumbai-76, rsinha@civil.iitb.ac.in*

Abstract

Quantification and classification of structural damage in RC buildings due to earthquakes is of prime importance for post-earthquake safety assessment. Vulnerability assessment and loss estimation to simulate the consequences of future earthquakes also rely on damage prediction of buildings. Seismic damage index, which evaluates incremental seismic damage from undamaged to completely damaged condition on a scale from zero to one or more, has been widely used to classify damage to buildings. A well-calibrated seismic damage index also allows the designer of a new building to choose failure mechanisms by supressing undesired failure modes. It can also help to provide rapid evaluation of safety of buildings after an earthquake. In this paper a comprehensive seismic damage index representing complete range of damage and capable of identifying wide range of moderate damage states of RC member has been presented. The parameters of proposed seismic damage index are calibrated by means of observable member damage states featuring specific residual seismic capacity. In this study, the observable member damage states are quantified with extreme fiber compressive strain by simulating experiments in PEER database. Observations from quasi-cyclic analyses of column specimens, covering entire range of member properties, have been used to quantify reduction in strength. The proposed seismic damage index ensures identification of wide range intermediate damage states and represents a significant improvement over prevalent damage indices.

Keywords: Seismic damage index, damage assessment, seismic damage states

1. Introduction

A large number of reinforced concrete (RC) buildings are damaged due to earthquakes that occur in different parts of the world every year. Building damage due to earthquakes is the primary cause of casualties and economic losses. There are a number of reasons for building damage, viz. the seismic codes may be deficient resulting in lower than required design force, design compliance with codes may be inadequate, the building construction may be deficient or the actual earthquake force may exceed the design values. For instance, advances in knowledge of seismic hazard during the last few decades have resulted in increase in seismic force requirement in design codes in several different countries including in India. In these situations, older buildings are deficient from current design codes even if they were designed and constructed to comply with prevalent standards at the time of their construction. Such buildings are likely to perform poorly in design-level earthquake events arising out of an improper understanding of seismic hazard in the past.

In conventional practice, when buildings are analytically evaluated to assess their extent of deficiencies considering the latest estimation of seismic hazard, say for retrofitting decisions, the prevalent assessment methods are primarily based on determination of seismic damage indices. These seismic damage indices, whose value vary between zero and one or more, are found to accurately predict the vulnerability of buildings when they are likely to remain undamaged (index value close to zero) or are likely to experience extensive damage (damage index value close to unity or higher). However, the available damage indices are not found suitable to differentiate between different levels of moderate damage [1, 2].

A well-designed RC building dissipates input seismic energy by distributed hinge formation in beams and columns and thereby avoids early formation of collapse mechanism. The distributed damage patterns can be formed by several ways [1, 2] and their residual seismic capacity (safety margin for lateral resistance) is a function of magnitude and relative distribution of damage in beams and columns. From critical review and evaluation of available seismic damage indices [2], it has been found that in the situations where the building may experience moderate damage, the available damage indices are often unable to quantify the extent of the deficiency. This affects the accuracy of the vulnerability assessment and quality of decisions such as retrofitting requirement that is based on the assessment. These damage index-based methods therefore also need to be revised in order to more accurately assess moderate damage to RC buildings. In this paper, a seismic damage index that is capable of accurately representing the complete range of damage states and capable of identifying a wide range of moderate damage states has been presented.

2. Proposed Member Seismic Damage Index

The linear combination of deformation and energy terms in widely used Park and Ang [3] damage index is unable to represent slight to moderate damage states. Bracci *et al.* [4] proposed a seismic damage index with a non-linear combination of deformation and normalised hysteretic energy terms. This formulation has been used a basis to develop new seismic damage index. The proposed seismic damage index is given as,

$$D_{proposed} = D_1 + D_2 - D_1 D_2 \text{ with } D_1 = \frac{\phi_m}{\phi_f} \text{ and } D_2 = \beta \frac{\int dE}{C_p \phi_y M_y} \tag{1}$$

where, ϕ_m, ϕ_y and ϕ_f represent maximum, yield and ultimate curvature of the member. Parameters M_y and $\int dE$ represent yield moment and dissipated hysteretic energy, respectively. D_1 is the deformation component of the damage index, captures initiation of damage state, and D_2 captures reduction in strength caused by damage accumulation due to cyclic loading. The damage component D_1 has been defined in terms of curvature instead of rotation, as curvature is directly related to extreme fiber compressive strain. In present study, extreme fiber compressive strain has been used for identification of different damage states (discussed later in section 2.1). Yield moment and curvature are defined with reference to first yield of reinforcement. Control parameter (C_p) maps incremental damage under cyclic loading, represented by normalised hysteretic energy and strength reduction factor β, between limiting damage index values. Parameter β is evaluated for observed loss in strength

during quasi-cyclic testing at collapse state of the member. In this study, the following equation proposed by Park *et al.* [5] has been used to estimate reduction in strength,

$$\beta = \left\{ 0.37\eta 0 + 0.36 \left(\frac{\rho_t f_y}{0.85 f_c} - 0.2 \right)^2 \right\} 0.9^{\rho_w} \tag{2}$$

In the proposed formulation, damage component D_1 ensures specific value of seismic damage index at particular damage state; while damage component D_2 maps accumulation of the damage in between values of damage index at successive damage states using control parameter C_p. Therefore for known values of parameter D_1 at successive moderate damage states, control parameter C_p is estimated as,

$$(D_2)_{\text{ModerateDS}} = \frac{(D)_{\text{at end of Moderate DS}} - (D_1)_{\text{at start of Moderate DS}}}{1 - (D_1)_{\text{at start of Moderate DS}}} \tag{3}$$

$$C_p = \beta \frac{\int dE}{M_y \phi_y (D_2)_{\text{ModerateDS}}} \tag{4}$$

Parameter $\int dE$ represents amount of hysteretic energy dissipated during cyclic loading before reaching next damage state. Fig. 1 illustrates estimation of control parameter C_p at moderate damage state on idealised moment-curvature relationship. The reduction in strength at intermediate damage states is assumed to be proportional to reduction in strength at ultimate state estimated by parameter β (Eq. 2).
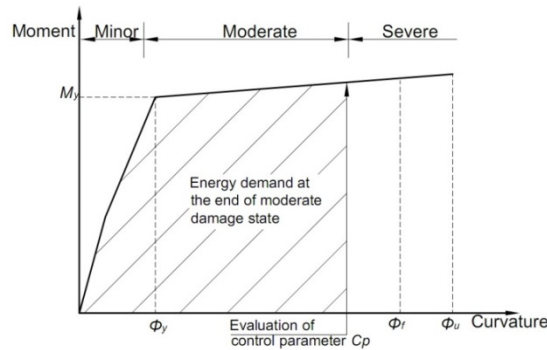
Fig. 1 – Control Parameter C_p in damage component D_2 for proposed damage index
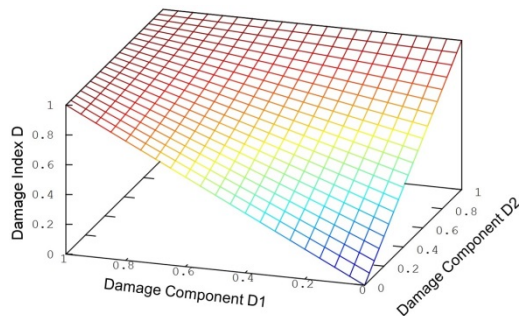
Fig. 2 – Variation of proposed damage index with respect to damage components D_1 and D_2

Fig. 2 shows a variation of proposed damage index (D) against the damage components D_1 and D_2. It can be seen that the proposed damage index function provides relatively large range of values between limits 0 and 1. The non-linear relationship between damage index D and damage components D_1 and D_2 provides flexibility to accommodate variation in hysteretic energy and provides a stable value of seismic damage index.

3. Capacity-Based Damage State Definitions

Damage to an RC frame member at the critical section is typically characterized by cracks in cover concrete, yielding of reinforcement, spalling of concrete cover, onset of core concrete crushing, buckling of longitudinal reinforcement and fracture of transverse/longitudinal reinforcement. In flexural-critical compression member subjected to repeated loading, minor to narrow shear cracks appear on the side face of the member as damage progresses between longitudinal cracking to crushing of concrete [6]. Widening of initial shear cracking occurs at crushing of core concrete or buckling of longitudinal reinforcement. Thus for flexural-critical beams and columns, shear cracking does not predominately affect load carrying capacity prior to buckling of longitudinal reinforcement. In a previous study, the authors [7] demonstrated that the onset of spalling and initial spalling (exposure of transverse reinforcement) occurring between minor and severe damage states, partially affect seismic capacity of the members. For individual members these damage conditions are repairable; but when several members experience initial to significant spalling, the seismic capacity of the complete building reduces substantially and repair may be uneconomical [8]. Therefore, the parameters of proposed seismic damage index reflecting occurrence and cyclic loading effects are calibrated at initiation spalling and significant spalling, in order to quantify combined effect of member damage states on seismic capacity of the complete building. It was also shown [7] that occurrence of various damage states is better characterised by extreme fiber compressive strains. Therefore, damage states are expressed in terms of extreme fiber compressive strain to calibrate control parameter, C_p.

3.1.1 Engineering limits for flexural damage states

Significant published literature is available on prediction of structural response at ultimate state, but very limited research has been carried out on identification and prediction of intermediate damage states. Berry and Eberhard [9] and Jiang *et al.* [10] expressed compressive strain, curvature and drift ratio at onset of significant spalling and initial bar buckling as a function of axial load ratio ($\underline{P/f_cA_g}$), span to depth ratio (L/D), longitudinal ($\rho_l f_y/f_c$) and confinement ratio ($\rho_w f_y/f_c$) using plastic hinge approximation and by enforcing equilibrium conditions on stress block, for flexure dominated rectangular columns in PEER [11] experimental database. The best fitted equations proposed by Berry and Eberhard [9] and by Jiang *et al.* [10], to estimate extreme fiber compressive strain at significant spalling, are as follows:

$$\varepsilon_{spall} = 0.001\left(1 - 0.0017\left(\frac{L}{D}\right)^{1.883}\right)\left(1 + 10.211\left(\frac{P}{f_c A_g}\right)^{-0.441}\right) \tag{5}$$

$$\varepsilon_{spall} = 0.00173 + 0.0256 K_e^4, \text{ where } K_e^4 = \frac{\left(1 - \sum_{i=1}^{n}\frac{\left(w_i'\right)^2}{6 b_{cor} h_{cor}}\right)\left(1 - \frac{s'}{2 b_{cor}}\right)\left(1 - \frac{s'}{2 h_{cor}}\right)}{\left(1 - \rho_{cc}\right)} \tag{6}$$

in which K_e is confinement effectiveness coefficient. b_{cor} and h_{cor} are the width and depth of the confined core of the section. s' is the spacing between stirrups, w_i' is the ith clear distance between adjacent longitudinal bars, ρ_{cc} is the ratio of area of longitudinal reinforcement to area of core of section. It should be noted that plastic hinge lengths used in these models were based on experimental data at failure. Therefore, the compressive strain values estimated from above equations slightly underestimates the actual values.

Berry and Eberhard [9] and Jinag *et al.* [10] predicted the mean value of compressive strain at onset of spalling/crushing as 0.004 and 0.005, respectively. These values are in the range with the mean compressive strain values proposed by Priestley [12], Lehman *et al.* [13] and Chen *et al.* [14].

Berry and Eberhard [9] proposed following equation to predict the compressive strains at initial bar buckling,

$$\varepsilon_{buckling} \; = \; 0.003\left(1+3.245\left(\frac{P}{f_c A_g}\right)^{0.058}\right)\left(1+4.027\left(\frac{\rho_l f_y}{f_c}\right)^{2.355}\right) \tag{7}$$

However, no expression has been proposed to estimate compressive strain at onset of spalling/crushing. Experimental column data available in PEER database [11] has been simulated in IDARC-2D 7.0 [15] to establish compressive strain at onset of spalling/crushing as described below.

3.1.2 Simulation of experimentally observed behaviour

Thirty-three experimental responses of rectangular columns with flexural failure mode, axial load ratio between 0.1 to 0.4, clear cover between 25 to 40 mm and displacements recorded either at crushing of concrete or significant spalling, were numerically simulated in IDARC-2D 7.0 [15]. The numerical simulations of experimental responses are described in detail in [7]. For each column, tri-linear moment curvature relationships were generated using stress strain relations of confined concrete and elasto-plastic with strain hardening stress-strain relationships of reinforcing steel.

3.1.3 Estimation of compressive strain at onset of spalling

From the numerical study, it is found that compressive strain at onset of spalling is not strongly correlated with column parameters. However, it was found that member response parameters are well correlated at onset of spalling and significant spalling, as shown in Fig. 3. Using these results, the following relationship is proposed to relate compressive strain at onset of spalling with the strain at significant spalling,

$$\varepsilon_{\text{initition of spalling/crushing}} \; = \; 0.5134 \times \varepsilon_{\text{significant spalling}} \; + 0.0004 \tag{8}$$

The mean and covariance of the ratio of strain estimated from Eq. (8) to experimental strain at onset of spalling are 0.86 and 34.42%. Thus, the proposed equation can accurately predicts compressive strain at onset of spalling. At greater damage levels, it is found that the equations proposed by Berry and Eberhard [9] (Eq. 5) can be used to predict compressive strain at significant spalling and bar buckling. The equation proposed by Jiang et al. (Eq. 6) overestimates the compressive strain values at significant spalling.

(a) Compressive strain   (b) Tip Deflection
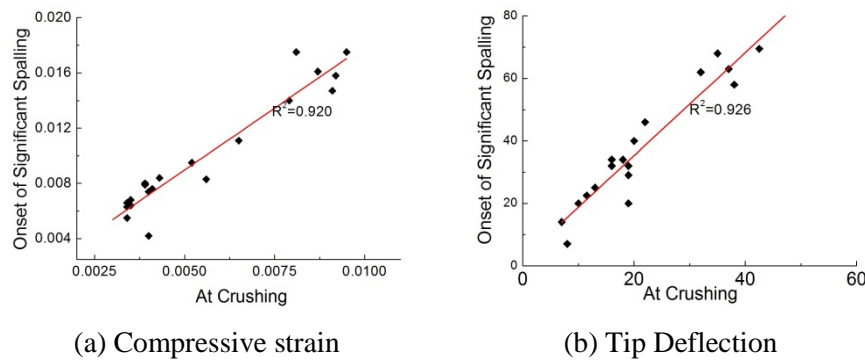
Fig. 3 – Comparison of response parameters at (a) onset of spalling, and (b) onset of significant spalling

4. Calibration of Proposed Member Seismic Damage Index

Calibration of proposed seismic damage index comprises of determination of control parameter. In this study, a database of cross sections with complete range of sectional properties has been generated for beams and columns. These have been analysed for the development of prediction equation for control parameters C_p in terms of cross-sectional parameters. The range of parameter values and their distribution used for random sample generation is summarised in Appendix A. Each random sample is modelled as a cantilever column with spread

plasticity hinges and analysed after applying ATC-24 quasi-cyclic loading pattern (Fig. 4) [16, 17]. ATC-24 [16] loading pattern employ energy demand consistent with that from moderate to high intensity earthquakes.
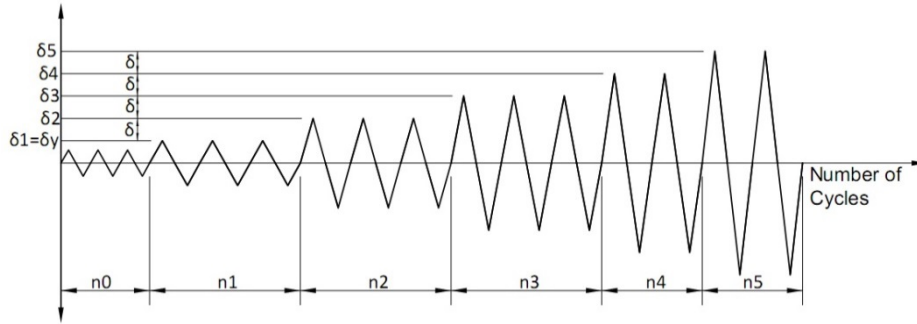
Fig. 4 – ATC-24 loading history for multiple-step test

For calibration of member seismic damage index, the occurrence of key damage states are identified from limiting values of extreme fiber compressive strains. Compressive strain at onset of spalling is determined from Eq. (8) and at initial buckling Eq. (7). Compressive strain at initiation of core crushing/ bar buckling is taken as twice the compressive strain at onset of significant spalling [13, 14]. Curvature ductility corresponding to extreme fiber compressive strains are estimated using developed moment curvature relationship.

4.1 Control parameter, C_p, for columns

The ultimate curvature ductility (ϕ_f) is used to scale the damage component D_1. Thus, the choice of ultimate curvature ductility, either at initiation of core crushing or at initial bar buckling, affects damage component D_1 and limiting value of member seismic damage index (D) for different damage states. Figs. 5 (a-b) represent the variation of curvature ductility ($\mu_\emptyset$) at initiation of core crushing/ bar buckling and initial bar buckling against axial load ratio. It is found that curvature ductility decreases monotonically from 6.99 to 3.77 and 10.03 to 5.64 due to increase in axial load ratio from 0.1 to 0.35 for both the cases. The constant value of curvature ductility of 6, corresponding to mean curvature ductility at initiation of core crushing, overestimates curvature ductility for lower story columns but underestimates the same for upper story columns. Nevertheless, this approximation simplifies the estimation of seismic damage index and is found to provide reasonable accuracy and has been adopted in the study. The control parameter C_p has been separately calibrated by setting damage states corresponding to initiation of core crushing (Case 'a'), initial bar buckling (Case 'b') and constant curvature ductility of 6 (Case 'c') that corresponds to initiation of core crushing. These ultimate states have been chosen so as to provide the ability of proposed seismic damage index to differentiate intermediate damage states for members as well as for buildings.

For random samples, mean values of curvature ductility at spalling, initial spalling, initiation of core crushing/ bar buckling and initial bar buckling are 2.64, 4.16, 6.26 and 9.49, respectively. The mean values of damage component D_1 at start and end of moderate damage states for Case 'a' are 0.42 and 0.67, respectively and those for Case 'b' are 0.28 and 0.44, respectively. For Cases 'a' and 'b', damage component D_2 is estimated individually for each random sample from actual curvature ductility at spalling, initial spalling and initiation of core crushing or initial buckling, as

$$D_2 = \frac{(D_1)_{\text{at initial spalling}} - (D_1)_{\text{at crushing}}}{1 - (D_1)_{\text{at crushing}}} \tag{9}$$

For Case 'c', mean values of damage component D_1 at start and end of moderate damage states with reference to average value of ultimate curvature ductility ($\phi_f = 6$) are 0.44 and 0.69, respectively. For these values of damage component D_1, value of damage component D_2 is 0.45. Thus, control parameters C_p. are evaluated for constant value of 0.45.
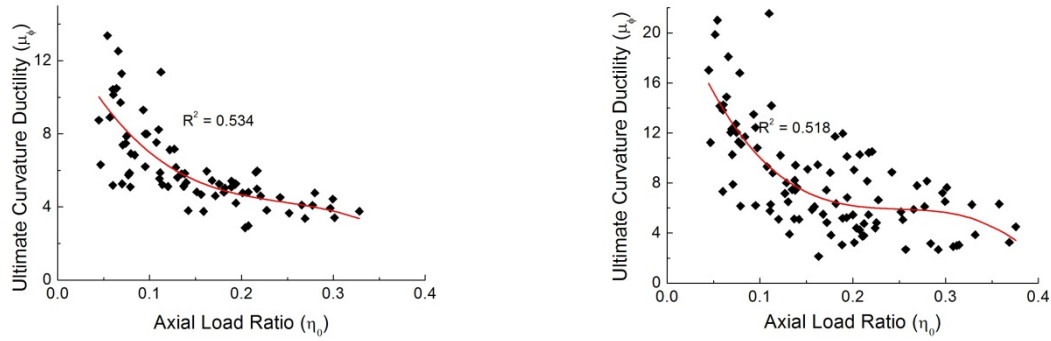
(a) At initiation of core crushing/ bar buckling   (b) At initial bar buckling

Fig. 5 – Variation of curvature ductility and against axial load ratio

Mean displacement ductility at crushing and initial spalling are found to be 2.20 and 3.28, respectively. These displacements occur in the first peak of n3 cycle and at the first peak of n4 cycle, respectively. Therefore, control parameters C_p are estimated for known energy dissipated during n0 to n3 cycles and the value of damage component D_2. If energy demand is more than that imposed by quasi-cyclic loading and maximum deformation demand is at initial spalling, the proposed seismic damage index exceeds moderate damage state and indicates severe damage state.

For all the above three cases, the control parameters (C_p) and ultimate curvature ductility (μ_ϕ) have been estimated as functions of member cross section properties using regression analyses and are given below.

a. For initiation of core crushing/ bar buckling as ultimate curvature ductility:

$$\text{Control parameter, } C_p = 21.49\eta_0 + \rho_w^{-0.052} - 2.248\left(\frac{\rho_l f_y}{0.85 f_c}\right) \tag{10}$$

$$\text{Ultimate curvature ductility, } \mu_\phi = \left(0.445\eta_0^{-0.896} + \left(\frac{\rho_w f_y}{0.85 f_c'}\right)^{0.019}\right)\left(\frac{\rho_l f_y}{0.85 f_c}\right)^{-0.338} \tag{11}$$

b. For initial buckling as a ultimate curvature ductility:

$$\text{Control parameter, } C_p = \left(100.694\eta_0 + 173.32\rho_w\right)\left(\frac{\rho_l f_y}{0.85 f_c}\right)^{0.884} \tag{12}$$

$$\text{Ultimate curvature ductility, } \mu_\phi = \left(1.305\eta_0^{-0.917} + \left(\frac{\rho_w f_y}{0.85 f_c}\right)^{0.114}\right)\left(\frac{\rho_l f_y}{0.85 f_c}\right)^{0.182} \tag{13}$$

c. For average curvature ductility at initiation of core crushing/ bar buckling:

$$\text{Control parameter, } C_p = \left(16.72\eta_0 + \rho_w^{0.169}\right)\left(\frac{\rho_t f_y}{0.85 f_c}\right)^{-0.310} \tag{14}$$

Table 1 summarises mean, maximum and minimum values of proposed damage index at the start and end of moderate damage states for Cases 'a', 'b' and 'c'. To examine the ability of proposed control parameter in mapping cyclic loading effect, seismic damage index at the end of moderate damage state are estimated by

adding damage component D_2, estimated from proposed control parameters (C_p) to values of damage component D_1 at yield and at the start of moderate damage state. The mean, maximum and minimum values of damage component D_1 (limiting value of damage index) at the start and end of moderate damage states are summarised in Table 1. Damage index at the start of moderate damage state is also evaluated by adding damage component D_2 estimated from proposed control parameters (C_p) to value of damage component D_1 at yield.

Table 1 –Damage index values at different damage states estimated from prediction equation for C_p, for columns

		Damage Component D_1			Damage Index D		
		At yield disp. (1st peak of n1)	Start of Mod. DS	End of Mod. DS	Start of Mod. DS wrt yield disp	End of Mod. DS wrt Start of Mod. DS disp	End of Mod. DS wrt yield disp
Case 'a' Eqs. (10) and (11)	Mean	0.192	0.511	0.799	0.390	0.784	0.661
	Std. Dev	0.007	0.110	0.180	0.153	0.186	0.296
	Min	0.086	0.284	0.439	0.226	0.383	0.293
	Max	0.355	0.794	1.22	0.946	1.329	1.737
Case 'b' Eqs. (12) and (13)	Mean	0.136	0.396	0.604	0.277	0.566	0.439
	Std. Dev	0.059	0.207	0.308	0.183	0.272	0.320
	Min	0.046	0.116	0.187	0.064	0.173	0.107
	Max	0.325	1.092	1.647	0.857	1.111	1.318
Case 'c' Eq. (14)	Mean	0.167	0.440	0.693	0.330	0.657	0.588
	Std. Dev	0.010	0.193	0.320	0.156	0.203	0.244
	Min	0.167	1.130	1.940	1.44	0.264	0.234
	Max	0.165	0.176	0.273	0.202	1.049	1.370

The mean values of proposed seismic damage index at the initiation of spalling at peak displacement (damage component D_1) and estimated with reference to yield displacement are 0.511, 0.390 and 0.396, 0.277, for Cases 'a' and 'b' respectively. Similarly, the mean values at the initial spalling estimated from peak displacement (damage component D_1), with reference to yield displacement, initiation of spalling are 0.799, 0.661, 0.781 and 0.604, 0.439, 0.566, for Cases 'a' and 'b', respectively. Thus for both Cases 'a' and 'b', the proposed control parameters C_p map deterioration under cyclic loading between damage index values at the start and end of moderate damage states reasonably well.

From Table 1 it is also observed that the proposed seismic damage index formulated with ultimate curvature ductility at initiation of core crushing/ bar buckling (Case 'a') renders higher values compared to those formulated with ultimate curvature ductility at initial bar buckling (Case 'b'), for slight to moderate damage states.

For Case 'c', the mean value damage component D_1 at the initial spalling and mean damage index at initial spalling estimated with reference to yield displacement, and initiation of spalling are 0.693, 0.588, and 0.657. From Table 1, it is further observed seismic damage index estimated from average curvature ductility

(Case 'c') are slightly lower compared to seismic damage index estimated from actual (Case 'a') values of curvature ductility. However, the use of average curvature ductility ($\phi_f = 6$), significantly reduces computational effort of estimating ultimate curvature ductility for individual members.

4.2 Control parameter C_p for beams

Equations predicting compressive strain at key damage states have been developed from experimental observations of columns with axial load ratios between 0.05 and 0.4. Such explicit relationships cannot be developed for beam members due to lack of experimental observations in the database. Generally, beams are treated as columns with very low axial load ratio (of the order 0.01 to 0.05). For beams, occurrence of key damage states is generally governed by amount of tension side reinforcement. For axial load ratio (η_0) of 0.05, mean curvature ductility at initiation of core crushing/ bar buckling and initial bar buckling, observed in Figs. 5(a-b), are 9.67 and 15.2.

The authors [7] correlated key damage states with residual and maximum crack widths. For simulated PEER experiments [11], the mean value of maximum crack width at initiation of spalling was observed as 2.5 mm. Thus, for beams, initiation of spalling is identified corresponding to maximum crack width of 2.5 mm. As the response parameters at successive intermediate damage states are well-correlated, limiting value of compressive strain at significant spalling is taken as 2 times compressive strain at 2.5 mm crack width.

The mean values of compressive strain and curvature ductility at crack width of 2.5 mm (initial crushing/spalling) obtained from 173 random samples are 0.0031 and 3.67. The mean value of curvature ductility at initial spalling (corresponding to compressive strain value 2 times strain at 2.5 mm crack width) is 6.58. Behaviour of curvature ductility at initiation of core crushing/ bar buckling estimated from Eq. (11) and at compressive strain limit (2 times strain at 2.5 mm crack width) against tension reinforcement ratio has been found to be identical. Mean values of curvature ductility at 2 times strain at 2.5 mm crack width and as per Eq. (13) are 8.67 and 9.79, respectively. Similar to the case of columns, the control parameters for beams are evaluated for the three cases. For Case 'a', the curvature ductility for initiation of core crushing/ bar buckling are determined from Eq. (11) for axial load ratio of 0.05. For Cases 'b' and 'c' cases control parameters are evaluated for ultimate curvature ductility of 15 and 10 corresponding to initial buckling and initiation of core crushing, respectively. For Cases 'a' and 'b', damage component D_2 (Eq. 9) is estimated from actual curvature ductility at spalling, initial spalling and initiation of core crushing or initial buckling, for each random sample. For Case 'c', the mean values of damage component D_1 for average curvature ductility ($\phi_f = 10$) at start and end of moderate damage states are 0.267 and 0.657, respectively. Thus, the control parameters C_p are evaluated for constant value of 0.53. In Case 'c', ultimate curvature ductility of 10 has been chosen to ensure value of damage component D_1 as 0.67, at the end of moderate damage state.

For all random beam samples, strength deterioration parameter β has been evaluated using Eq. (2) with axial load ratio (η_0) as 0.05. The widely used Gergely and Lutz [18] crack-width formula has been used to estimate maximum crack width.

The mean displacement ductility at spalling (start of moderate DS) and initial spalling (end of moderate DS) are 2.42 and 5.69, which occur in the first peak of n3 and at the first peak of n6 cycles, respectively. Therefore control parameter C_p has been estimated as per Eq. (9) for known energy dissipated during n0 to n5 cycles and value of damage component D_2. The control parameters are strongly correlated with tension reinforcement ratio, compared to confinement reinforcement ratio. The following equations are proposed to determine control parameters, C_p.

a. For initiation of core crushing/ bar buckling as a ultimate curvature ductility:

$$\text{Control parameter, } C_p = 3.855 - 14.680\left(\frac{\rho_t f_y}{0.85 f_c}\right) + 33.970\left(\frac{\rho_t f_y}{0.85 f_c}\right)^2 \tag{15}$$

b. For initial buckling as a ultimate curvature ductility:

$$\text{Control parameter, } C_p = 7.950 - 42.73\left(\frac{\rho_t f_y}{0.85 f_c}\right) + 111.11\left(\frac{\rho_t f_y}{0.85 f_c}\right)^2 \qquad (16)$$

c. For average curvature ductility at initiation of core crushing/ bar buckling:

$$\text{Control parameter, } C_p = 4.255 - 17.610\left(\frac{\rho_t f_y}{0.85 f_c}\right) + 42.109\left(\frac{\rho_t f_y}{0.85 f_c}\right)^2 \qquad (17)$$

Table 2 –Damage index values at different damage states estimated from prediction equation for C_p, for beams

		Damage Component D_1			Damage Index D		
		At yield disp. (1st peak of n1)	Start of Mod. DS	End of Mod. DS	Start of Mod. DS wrt yield disp	End of Mod. DS wrt Start of Mod. DS disp	End of Mod. DS wrt yield disp
Case 'a' Eq. (15)	Mean	0.121	0.435	0.783	0.275	0.727	0.580
	Std. Dev	0.024	0.107	0.150	0.071	0.119	0.172
	Min	0.064	0.411	0.410	0.172	0.507	0.265
	Max	0.171	1.277	1.247	0.578	1.075	1.132
Case 'b' Eq. (16)	Mean	0.067	0.243	0.439	0.147	0.435	0.307
	Std. Dev	0.001	0.036	0.073	0.042	0.100	0.097
	Min	0.067	0.178	0.291	0.100	0.259	0.153
	Max	0.067	0.361	0.676	0.266	0.727	0.604
Case 'c' Eq. (17)	Mean	0.010	0.365	0.658	0.245	0.663	0.531
	Std. Dev	0.003	0.054	0.109	0.074	0.137	0.171
	Min	0.010	0.267	0.437	0.134	0.410	0.197
	Max	0.011	0.542	1.0013	0.524	1.051	1.068

Table 2 summarises mean, maximum and minimum values of damage index at the start and end of moderate damage states for Cases 'a', 'b' and 'c' of beam specimens. The mean values of proposed seismic damage index at the initiation of spalling at peak displacement (damage component D_1) and estimated with reference to yield displacement are 0.435, 0.275 and 0.243, 0.147, for Cases 'a' and 'b', respectively. Similarly, the mean values at initial spalling estimated at peak displacement (damage component D_1) and estimated with reference to yield displacement, initiation of spalling are 0.783, 0.580, 0.727 and 0.439, 0.307, 0.435, for Cases 'a' and 'b', respectively. Thus, the proposed control parameter, C_p, maps deterioration caused by cyclic loading between damage index values at the start and end of moderate damage states. Similar to the case with columns,

the proposed seismic damage index with ultimate curvature ductility at initiation of core crushing/ bar buckling yields higher values compared to ultimate curvature ductility at initial buckling. For Case 'c', mean value at the initial spalling estimated from peak displacement (damage component D_1) and estimated with reference to yield displacement, initiation of spalling are 0.658 and 0.531, 0.663, respectively. Thus, damage index estimated from constant average curvature ductility ($\phi_f = 10$) yields slightly lower values compared to actual values of curvature ductility.

5. Limiting Values of Proposed Seismic Damage Indices

The proposed seismic damage index varies between 0 to 0.44 for minor to slight damage levels, 0.44 to 0.66 for moderate damage state and higher than 0.66 for severe damage state, for both columns and beams.

6. Conclusions

The paper discusses a new generalised member damage index, which renders large range of values to capture intermediate damage states. The proposed damage index captures initiation of all possible damage states occurring between undamaged and collapsed states, and is also capable of mapping the cumulative damage caused by cyclic loading between successive damage index values. The parameters of proposed seismic damage index are calibrated by means of observable member damage states, featuring specific residual seismic capacity. In this regard, the observable member damage states are correlated with extreme fiber compressive strain using PEER experimental database. These relationships are used to calibrate control parameter C_p of proposed seismic damage index at moderate damage states. For member seismic damage indices, the proposed damage index varies between 0-0.66 for undamaged to moderate damage states and is >0.66 for severe damage states.

Appendix A: Generation of Random Samples

Random samples are generated by considering variations in axial load ratio (η_0), longitudinal steel reinforcement ratio (ρ_l), tension-side steel reinforcement ratio (ρ_t) and member dimensions. Variation in span to depth (l/d) ratio has not been considered, as response of well-detailed member is dominated by flexural deformation. Axial load ratio (η_0) and longitudinal steel reinforcement ratio (ρ_l) are assumed to be uniformly distributed. Discrete random numbers are generated for column size, number of longitudinal reinforcement bar, stirrup diameter, concrete characteristic strength (f_{ck}) and yield strength of longitudinal reinforcement (f_y). Domain values of these parameters used to generate random samples of uniform distribution are summarised in Table 3.

For columns, axial load ratio and longitudinal reinforcement are assumed to be uniformly distributed between 0.05 to 0.4 and 0.01% to 0.03%, respectively. For beams tension-side steel reinforcement is assumed to be uniformly distributed between 0.75% and 2.5%.

Table 3 - Values of member properties to generate random samples

Column property	Uniform distributed values
Member size (mm)	350, 400, 450, 500, 550
Number of longitudinal reinforcement bars	8, 10, 12, 14
Stirrup Diameter (mm)	8, 10, 12
Concrete Characteristic Strength (f_{ck}) (MPa)	25, 30, 35, 40
Yield strength of longitudinal reinforcement (f_y) (MPa)	30, 35, 40, 45, 50

7. References

[1] Shiradhonkar SR, Sinha R (2012): Seismic damage index for classification of structural damage – closing the loop. *15th World Conference on Earthquake Engineering*, Lisbon, Portugal.

[2] Shiradhonkar SR, Sinha R (2012): Detailed evaluation of available seismic damage indices. *ISET Golden Jubilee Symposium*, Roorkee, India.

[3] Park YJ, Ang AHS (1985): Mechanistic seismic damage model for reinforced concrete. *Journal of Structural Engineering, ASCE*, **111** (4), 722-739.

[4] Bracci JM, Reinhorn AM, Mander JB, Kunnath SK (1989): Deterministic model for seismic damage evaluation of RC structures. *Technical Report NCEER-89-00333*, National Center for Earthquake Engineering Research, SUNY, Buffalo, USA.

[5] Park YJ, Reinhorn AM, Kunnath SK (1988): Seismic damage analysis of reinforced concrete. 9th *World Conference on Earthquake Engineering*, Tokyo-Kyoto, Japan.

[6] Bearman CF (2012): Post-earthquake assessment of reinforced concrete frames. *PhD Thesis*, University of Washington, USA.

[7] Shiradhonkar SR, Sinha R (2014): Validation of seismic damage states for reinforced concrete buildings. *10th US National Conference on Earthquake Engineering*, Anchorage, USA.

[8] Shiradhonkar SR, Sinha R (2014): Seismic global damage states for post-earthquake visual safety assessment of reinforced concrete buildings. *15th Symposium on Earthquake Engineering (15SEE)*, IIT Roorkee, Roorkee, India.

[9] Berry M, Eberhard MO (2004): Performance models for flexural damage in reinforced concrete columns. *Technical Report*, Pacific Earthquake Engineering Research Center, College of Engineering, University of California, USA.

[10] Jiang H, Lu X, Kubo T (2010): Damage displacement estimation of flexure-dominant RC columns. *Advances in Structural Engineering*, **13** (2), 357-368.

[11] Berry M, Parrish M, Eberhard MO (2004): PEER structural performance database user's manual (version 1.0). *Technical Report*, University of California, Berkeley, USA.

[12] Priestley MJN (2000): Performance based seismic design. *New Zealand Society for Earthquake Engineering*, **33** (3), 325-346.

[13] Lehman D, Moehle J, Mahin S, Calderone A, Henry L (2004): Performance based seismic design. *Journal of Structural Engineering, ASCE*, **130** (6), 869-879.

[14] Chen L, Lu X, Jiang H, Zheng J (2009): Experimental investigation of damage behavior of RC frame members including non-seismically designed columns. *Earthquake Engineering and Engineering Vibration*, **8** (2), 301-311.

[15] Reinhorn AM, Roh H, Sivaselvan M, Kunnath S, Valles R, Madan A, Li C, Lobo R, Park Y (2009): IDARC 2D Version 7.0: A Program for the Inelastic Damage Analysis of Buildings. *Technical Report*, SUNY Buffalo, New York, USA.

[16] ATC-24 (1992): Guidelines for cyclic seismic testing components of steel structures. *Technical Report*, Applied Technology Council, Redwood City, California, USA.

[17] Krawinkler H (1996): Cyclic loading histories for seismic experimentation on structural components. *Earthquake Spectra*, **12** (1), 1-12.

[18] Gergely P, Lutz LA (1968): Maximum Crack-Width in Reinforced Concrete Flexural Members. Causes, Mechanism, and Control of Cracking in Concrete. *ACI*, **SP-20**, 87-117.